

Yoderite, a new hydrous magnesium iron aluminosilicate from Mautia Hill, Tanganyika.

(With Plate XI.)

By DUNCAN MCKIE, M.A., B.Sc., A.R.I.C., F.G.S.

Dept. of Mineralogy and Petrology, Downing Place, Cambridge.

With chemical analyses by A. J. RADFORD, B.Sc., F.R.I.C.

Geological Survey, Causeway, Salisbury, Southern Rhodesia.

[Read 6 November 1958.]

Summary. Yoderite occurs as a major constituent in a quartz-kyanite-talc schist, and is a high-pressure phase formed by the reaction $Ky + Tc \rightarrow Yd + Qu$. The monoclinic unit-cell, a 8.10 Å., b 5.78 Å., c 7.28 Å., β 106°, space-group $P2_1$ or $P2_1/m$, contains approximately $(Mg_{2.0}Ca_{0.2}Fe_{0.5}Al_{5.3})Si_{4.0}O_{17.6}(OH)_{2.4}$. The structure appears to be related to that of kyanite, with which the mineral is intergrown; it is not an analogue of staurolite. The three strongest powder lines are 3.50 Å. vs. 3.03 Å. vs. 2.61 Å. s. Specific gravity 3.39. Subsidiary reflections, similar to those of the intermediate plagioclases, have indices with non-simple fractional values of k . Optical properties are α 1.689 pale Prussian blue, β 1.691 indigo, γ 1.715 light olive-green, absorption $\beta > \alpha > \gamma$, $2V_\gamma$ 25°, optic axial plane {010}, γ :{001} $\approx 7^\circ$ in the obtuse angle β . An interpretation of the colour on the electron-exchange hypothesis $Fe^{2+} \rightleftharpoons Fe^{3+} + e^-$, is suggested. A kinetic study has been made of the disappearance of the subsidiary reflections in the range 700° C. to 820° C.; further heating to 850° C. produces the metastable appearance of mullite, and at temperatures above 1100° C. the equilibrium anhydrous assemblage andialite + sapphire appears.

YODERITE, a spectacular purple mineral, occurs in a quartz-yoderite-kyanite-talc schist at Mautia Hill (6° 8½' S., 36° 29' E.), 6 miles north-east of the former Groundnut Scheme headquarters at Kongwa, Mpwapwa District, Central Province, Tanganyika Territory. The general geology of the district has been described by Temperley (1938), who regarded (p. 40) the yoderite-bearing rocks as glaucophane-kyanite-magnetite-muscovite-quartz schists and observed that 'glaucophane' always surrounds kyanite; a more detailed account of the petrology of Mautia Hill is in course of preparation by the author and J. R. Harpum. Mautia Hill is an east-west ridge, 2 miles long by ½ mile wide, of metamorphic rocks of the Usagaran System (Archaean), consisting of steeply dipping units of east-west striking crystalline lime-

stone, quartzite, piemontite-quartzite, kyanite-biotite gneiss, quartz-yoderite-kyanite-talc schist, and amphibolite, the whole completely surrounded by the poorly exposed migmatites of the Kongwa plains. No recognizable continuation of the distinctive Mautia succession appears to occur either to the east or the west.

The mineral is named in honour of Dr. H. S. Yoder, Jr., of the Geophysical Laboratory, Carnegie Institution of Washington, who first studied experimentally the central part of the $\text{MgO-Al}_2\text{O}_3\text{-SiO}_2\text{-H}_2\text{O}$ system, within which 92 % of the composition of yoderite lies.

Yoderite has in the past been mistaken for glaucophane and for dumortierite, the characteristic pleochroism of which is closely similar; it was first recognized as a distinct mineral by its X-ray powder pattern.

Petrography. The quartz-yoderite-kyanite-talc schist is composed of coarse interlocking, often curved, flakes of talc with interstitial patches of quartz, exhibiting strain shadows; large irregularly margined grains of yoderite enclose random flakes of talc and some quartz. The general aspect of the rock is shown in pl. XI, fig. 1. A constant feature is the presence within each yoderite grain of relicts of kyanite (pl. XI, fig. 3), and kyanite occurs rimmed by yoderite (pl. XI, fig. 4). Quartz and talc occur on the outer margins of yoderite grains; the replacement of talc by yoderite is shown in pl. XI, fig. 2. Small rounded grains of hematite are randomly distributed through all other minerals. Yoderite and kyanite both contain large rounded quartz inclusions (pl. XI, figs. 3, 4); less regular patches of quartz also occur within yoderite grains. Every yoderite grain, however large and poikiloblastic, is optically a single crystal and all the kyanite relicts within it are in parallel orientation. Yoderite invariably separates talc from kyanite; assemblages present are quartz-yoderite-kyanite-hematite and quartz-yoderite-talc-hematite.

The proportions of quartz and talc vary markedly from the common talc-rich schistose type to a talc-yoderite-kyanite-quartzite. Yoderite has been studied from two specimens, a talc-rich type bearing the Geological Survey of Tanganyika number JH 2563/2 and a quartz-rich type numbered JH 2563/14.

Chemical composition.

Yoderite from specimen JH 2563/2 was freed from talc and quartz by centrifugal separation of -60 mesh +120 mesh material in methylene iodide, followed by electromagnetic removal of hematite, repeated electromagnetic separation of weakly magnetic yoderite from kyanite,

and finally hand-picking. Some 2 g. were available for the main analysis and a further portion, crushed to -90 mesh +120 mesh, was very carefully picked free of hematite-contaminated grains for the iron determinations.

The analysis is set down in table I and corresponds to the formula $(Mg_{2.0}Ca_{0.2}Fe_{0.5}Al_{5.3})Si_{4.0}O_{17.6}(OH)_{2.4} \cdot H_2O +$ was determined by direct weighing of the water evolved on ignition at 1100° C. in a tube furnace. The marked insolubility of yoderite made the determination of FeO

TABLE I. Chemical composition and unit-cell contents of yoderite.

	1.	2.		3.	4.	
SiO ₂ ...	36.12	36.07	Si ⁴⁺ ...	0.6006	4.00	} 4.03
TiO ₂ ...	0.35	0.35	Ti ⁴⁺ ...	0.0044	0.03	
Al ₂ O ₃ ...	41.06	41.00	Al ³⁺ ...	0.8041	5.35	} 8.06
Fe ₂ O ₃ ...	0.50	0.50	Fe ³⁺ ...	0.0063	0.04	
FeO ...	4.82	4.81	Fe ²⁺ ...	0.0670	0.45	} 20.00
MnO ...	0.32	0.32	Mn ²⁺ ...	0.0045	0.03	
MgO ...	12.23	12.21	Mg ²⁺ ...	0.3028	2.02	} 17.64
CaO ...	1.48	1.48	Ca ²⁺ ...	0.0262	0.17	
Na ₂ O ...	0.01	0.01	Na ⁺ ...	0.0003	—	} 20.00
K ₂ O ...	0.05	0.05	K ⁺ ...	0.0011	—	
H ₂ O+ ...	3.20	3.20	OH ⁻ ...	0.3552	2.36	} 20.00
H ₂ O- ...	0.05	—	O ²⁻ ...	2.6495	17.64	
	<u>100.19</u>	<u>100.00</u>				

1. Analysis of yoderite from specimen JH 2563/2. Analyst: A. J. Radford.
2. Analysis 1 recalculated to 100 % on an H₂O— free basis.
3. Atomic ratios.
4. Unit-cell contents corresponding to 20 anions per unit cell.

difficult; the method of Groves (1951, p. 183) proved unsatisfactory and I am indebted to Mr. J. H. Scoon¹ for a redetermination using Hey's (1941) micro-method, the result of which is quoted in table I. Cu, Pb, Co, Ni, B, and P were sought and found not to be present in significant amounts. Dr. S. R. Nockolds¹ confirmed the absence of Cu, Co, F, and B spectrographically.

Physical properties.

Yoderite occurs in anhedral, irregularly lath-shaped grains up to $\frac{1}{2} \times \frac{1}{4} \times \frac{1}{8}$ inches. Its hardness is 6 on Mohs' scale. Measurements of specific gravity by displacement of methylene iodide from a specific gravity bottle gave a value of 3.39. Refractive indices at 20° C. are α 1.689, β 1.691, γ 1.715 (all ± 0.002); and $2V$, 25° ($\pm 2^\circ$). The pleochroic

¹ Department of Mineralogy and Petrology, University of Cambridge.

scheme is α pale Prussian blue, β indigo, γ light olive-green, with absorption $\beta > \alpha > \gamma$. In the absence of crystal faces and good cleavages the orientation of the optical indicatrix had to be determined by direct reference to the chosen monoclinic crystallographic axes; optical direc-

TABLE II. X-ray powder data for yoderite.

<i>d</i> , Å.	<i>I</i> .	<i>d</i> , Å.	<i>I</i> .	<i>d</i> , Å.	<i>I</i> .	<i>d</i> , Å.	<i>I</i> .
4.64	w	1.97	m	1.219	vw	0.909	vvw
4.18	vvw	1.89	w	1.210	vw	0.893	vvw
3.87	vw	1.84	vvw	1.202	vw	0.891	vvw
3.83	vw	1.82	s	1.197	vw	0.888	vvw
3.63	w	1.752	vvw	1.175	vvw	0.883	vvw
3.50	vvs	1.727	m	1.166	vvw	0.863	vvw
3.34	vvw	1.698	vw	1.101	vvw	0.861	vvw
3.23	ms	1.647	vw	1.076	vwB	0.845	vvw
3.19	ms	1.610	w	1.058	vvw	0.843	vvw
3.07	vw	1.596	w	1.054	vvw	0.8375	vvw
3.03	vs	1.561	vvw	1.041	vvw	0.8360	vvw
2.91	ms	1.547	w	1.038	vvw	0.8306	vvw
2.72	vw	1.534	w	1.033	vw	0.8284	vvw
2.68	m	1.515	w	1.007	vw	0.8256	vvw
2.65	vw	1.499	wB	1.005	vvw	0.8232	vw
2.61	s	1.473	wB	0.999	w	0.8184	vvw
2.58	ms	1.451	m	0.997	vw	0.8165	vvw
2.46	ms	1.437	vw	0.985	vw	0.8142	vvw
2.41	vvw	1.415	w	0.983	vvw	0.8131	vvw
2.39	mw	1.399	mw	0.977	vvw	0.8110	vvw
2.36	w	1.382	vwB	0.973	vvw	0.8085	vvw
2.32	w	1.356	m	0.967	vw	0.8051	vvw
2.27	vw	1.340	vw	0.964	vvw	0.8029	vvw
2.24	msB	1.328	m	0.945	vw	0.8005	vvw
2.16	vw	1.298	vw	0.943	vvw	0.7979	vvw
2.11	vw	1.286	vvw	0.939	vw	0.7957	vvw
2.06	vvw	1.265	vvw	0.925	vvw	0.7865	vvw
2.00	s	1.240	vvw	0.915	vvw	0.7785	vvw

X-ray powder data for the analysed sample of yoderite (JH 2563/2). Relative intensities *I* were estimated visually. A camera of 19 cm. diameter and Cu-*K* α radiation were used.

tions in a grain were labelled by attaching glass fibres and the grain was then completely oriented by a zero-layer *b*-axis Weissenberg photograph. The optic axial plane is {010}, $\alpha \wedge a \approx 9^\circ$ and $\gamma \wedge c \approx 7^\circ$, both in the obtuse β -angle. Parting directions are [001] moderately good and {100} poor. Grains are elongated parallel to [010] and longitudinal sections can therefore be length fast or length slow.

X-ray powder data for yoderite are presented in table II; 112 lines were measured. The three strongest lines are: 3.50 Å. vvs, 3.03 Å. vs,

2.61 Å. s. The iron content of the mineral is not high enough to produce any serious fluorescent fogging with Cu- $K\alpha$ radiation.

X-ray crystallography.

In the single-crystal study of yoderite grains were used from specimens JH 2563/2 and JH 2563/14; no differences were observed in the diffraction patterns. The symmetry of a b -axis oscillation photograph and that of a zero-layer Weissenberg photograph about the b -axis show that the mineral is monoclinic. The unit-cell dimensions and space-group were determined from oscillation photographs about the a , b , and c axes, and from zero and fourth layer Weissenberg photographs about the a -axis. The unit-cell dimensions are a 8.10 Å., b 5.78 Å., c 7.28 Å. (all ± 0.05 Å.), and β 106° ($\pm 1^\circ$); $a:b:c = 1.402:1:1.259$. The only systematic absences were $0k0$ with k odd. Certain extra weak reflections that cannot be indexed on the lattice described above were observed on all overexposed photographs and will be discussed below. The space-group of the pseudo-lattice is therefore $P2_1$ or $P2_1/m$; a positive pyroelectric effect suggests that $P2_1$ is the more likely.

The unit-cell volume 328 Å.³ corresponds to the unit-cell contents shown in column 4 of table I, or to $\{X_2\text{Si}(\text{O},\text{OH})_5\}$, analogous to the aluminium silicate formula Al_2SiO_5 with some replacement of Al and O, all positions being occupied and no Si replaced. Al^{3+} is replaced essentially by Mg^{2+} , Fe^{2+} , Fe^{3+} , and Ca^{2+} , one-third of the Al^{3+} ions being replaced; the charge deficiency is compensated by the substitution of 2.35 OH^- for O^{2-} . The volume per oxygen atom is 16.4 Å.³, compared with 14.2 Å.³ in kyanite (where the oxygen ions are approximately in cubic close packing), 16.2 Å.³ in sillimanite, 15.2 Å.³ in staurolite, and 17.1 Å.³ in mullite increasing to 17.5 Å.³ in synthetic iron-rich mullites.

Yoderite is seen in thin-section to contain relicts of kyanite in constant optical orientation. An oscillation photograph of a composite grain about the b -axis of yoderite indicated b (yoderite) $\parallel c$ (kyanite), and a zero layer Weissenberg photograph about this common axis gave a complete account of the relative orientation, which is shown in fig. 1. Extra reflections on the Weissenberg photograph show that kyanite in this grain is twinned about the normal to $\{100\}$, a not uncommon twin law in kyanite. b 5.78 Å. of yoderite is similar and parallel to c 5.56 Å. of kyanite, representing the length of two octahedral groups in the aluminium-oxygen chains, a common feature of the unit cells of all the aluminium silicates; a 8.10 Å. for yoderite is similar and parallel to b 7.72 Å. for kyanite; c 7.28 Å. for yoderite is not dissimilar to $a \sin \beta$

6.96 Å. for kyanite. Thus the yoderite unit cell is expanded by about 5% in the a and c directions relative to kyanite, and by 4% in the direction of the aluminium-oxygen chains, b_Y being similar to the corresponding parameter a 5.74 Å. of sillimanite. Considerable structural similarity may thus be expected between yoderite and kyanite; chains of aluminium coordinated octahedrally to oxygen may be expected to

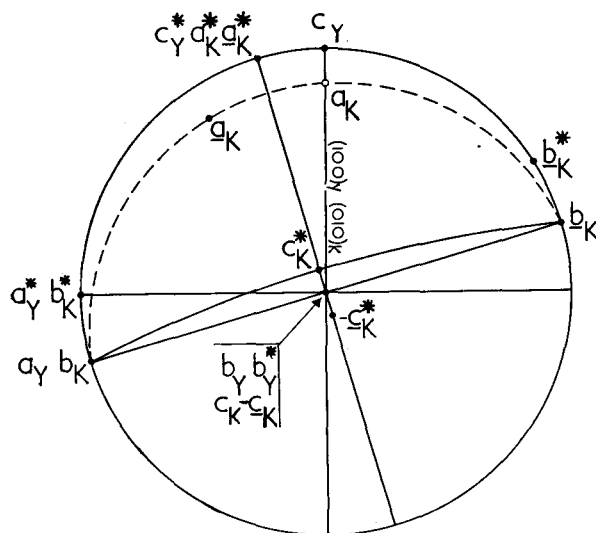


FIG. 1. Stereogram showing the relative orientation of yoderite (Y) and kyanite (K). Underlined symbols refer to the second individual of the kyanite twin.

run parallel to b , the chains being linked laterally by silicon in fourfold coordination and by aluminium probably in sixfold coordination as in kyanite. Aluminium, exhibiting sixfold coordination in both positions, may be designated Al_I in the chains and Al_{II} in the cross-linkages; the cations substituting for Al in yoderite all normally exhibit sixfold coordination and might therefore appear to replace Al in either position. The distribution of the 2.4 OH^- ions per unit cell may be random, but if the explanation of the colour of yoderite given below is correct and Weyl's (1951) interpretation of the pleochroic scheme of biotite is of general application the OH^- ions should be concentrated on planes perpendicular to the direction of minimum absorption γ , that is near $(\bar{1}06)$, which is parallel to $(6\bar{1}0)$ of kyanite, a plane, however, of no special significance in the kyanite structure.

Consideration of the atomic coordinates in kyanite (Naray-Szabo, Taylor, and Jackson, 1929) clarifies the structural relationship between yoderite and kyanite. Small displacements in the positions of atoms in the kyanite structure can give rise to a monoclinic $P2_1$ lattice, the largest adjustments being in the z -coordinates of Al in cross-linkages, Al_{III} and Al_{IV} of Naray-Szabo *et al.* The dimensions of the resultant unit-cell would be a' 6.96 Å., b' 7.72 Å., c 5.56 Å., β' 106°; it would be oriented with respect to the triclinic kyanite lattice in precisely the same way as yoderite was observed to be oriented in yoderite-kyanite intergrowths. The partial substitution of Mg²⁺ for Al³⁺ would appear to produce the requisite distortion, accompanied by an overall linear expansion of 4–5 %.

The orientation of staurolite with respect to kyanite (Naray-Szabo *et al.*, 1929) contrasts with that of yoderite in intergrowth with kyanite; c is a common direction in both cases, but the common plane is (100) of kyanite in the former and (010) in the latter instance. Fe²⁺ and OH⁻ ions lie on {010} planes in staurolite, which are parallel to the AlO₆ chains and therefore there is no significant (1 %) increase in chain length. The repeat distance normal to the Fe(OH)₂ layers, b_s 16.52 Å., is however of the order of 18 % greater than the corresponding dimension for two units of kyanite structure. The absence of such a strongly directed expansion, the difference in relative orientation, and crystallochemical considerations indicate that yoderite is not analogous to staurolite in its relationship to the kyanite structure.

Subsidiary reflections.

Sharp weak extra reflections occur between the layer lines on heavily exposed b - and c -axis but not on a -axis oscillation photographs. The separation of the subsidiary reflections from the principal layer lines was determined accurately and corresponds to $k = n \pm 0.165$, $n \pm 0.417$ and $l = n + \frac{1}{2}$; the values of the fractional indices may be expressed approximately, though perhaps without much significance, as $\frac{2}{12}$ (= 0.167) and $\frac{5}{12}$, corresponding to twelvefold multiplication of the b parameter with systematic absence of all but the $12n$ (strong), $12n \pm 2$, $12n \pm 5$ layer lines. Weissenberg photographs of the zero and fourth layers about the a -axis and of the k 1.417 layer about the b -axis were used to determine the positions of the subsidiary reflections in reciprocal space. Two types of reflections occur, type I with indices n , $n' \pm 0.417$, $n'' \pm \frac{1}{2}$, and type II with indices n , $n' \pm 0.167$, n'' . The diffraction pattern of yoderite is thus characterized by pairs of subsidiary reflections sym-

metrically separated by a translation corresponding to $0.083 b^*$ from absent reflections which would represent halving of b^* and c^* , and by pairs of subsidiary reflections disposed in an identical manner about the strongest principal reflections; the resemblance of this pattern to that exhibited by intermediate plagioclases and investigated in detail by Cole, Sörum, and Taylor (1951), and Gay (1956), is marked. Any dependence of the separation of the subsidiary reflections on composition cannot be investigated at present as all specimens of yoderite from Mautia Hill produce identical diffraction patterns. Any convincing attempt at explanation of the subsidiary reflections is difficult in a mineral whose structure is undetermined and in which possibilities of the occurrence of ordered sequences in the distributions of Al and Si, Mg and Al, OH and O occur. The very small atomic scattering factor of H, however, makes it unlikely that ordering of the OH distribution could give rise to the observed effects.

The assignment of Al atoms exclusively to sixfold positions and Si atoms to fourfold positions in kyanite provides a completely ordered structure in which no extensive substitution by other cations is known to occur, and it is not surprising to find a complete absence of subsidiary reflections on heavily overexposed c -axis oscillation photographs of kyanite. In staurolite Fe^{2+} and OH^- ions separate blocks of kyanite structure to produce a completely ordered structure, and subsidiary reflections failed to appear on a c -axis oscillation photograph heavily overexposed to $\text{Fe-}K\alpha$ radiation. Subsidiary reflections are lacking too on c -axis oscillation photographs of lusakite, which has a structure analogous to staurolite (Skerl and Bannister, 1934). Agrell and Smith (1957) have observed in mullite diffraction patterns certain weak non-integral reflections, which are similar to those of the intermediate plagioclases; such subsidiary reflections may be tentatively related to either the presence of Si and Al in ordered sequences in fourfold positions, or to some degree of ordering in the distribution of 39 O^{2-} between forty available positions, or both.

If the analogy between the inferred structure of yoderite and that of kyanite is as good as has been suggested, the possibility of the subsidiary reflections being due to Si-Al ordering may be ruled out because subsidiary reflections are not observed and such ordering cannot occur in kyanite; thus the subsidiary reflections observed in yoderite may be regarded as related to the presence of ordered sequences in the distribution of Mg and Al in equivalent or nearly equivalent positions.

Heat treatment. Single crystals were subjected to successive heatings so that each crystal had an effectively isothermal history. Temperatures were controlled by a platinum resistance thermometer and continuously recorded by a chromel-alumel thermocouple; a constancy of $\pm 5^\circ$ C. was maintained between successive heatings. Quenching by cooling in air to room temperature took < 3 minutes. After each heating the crystals were examined by oscillation photographs (15° oscillation) about the b -axis with the X-ray beam, accurately set by Laue photograph, in a standard orientation $\perp(403)$; this orientation causes the reciprocal lattice point corresponding to one of the strongest of the subsidiary reflections $1.1\cdot 417.\frac{1}{2}$ to be intersected by the sphere of reflection near the middle of the oscillation. The intensities of this reflection and of two principal reflections (assumed to be unaffected by heating) were measured by visual comparison with a linear intensity scale and the intensity I of reflection $1.1\cdot 417.\frac{1}{2}$ after heating at T° C. for t hours was expressed as a fraction of its initial intensity I_0 . As a check on the generality of the intensity variation of $1.1\cdot 417.\frac{1}{2}$, measurements were made of the intensity of the other strong subsidiary reflection $0.1\cdot 417.\frac{1}{2}$ for heatings at 730° C., and a similar variation was found. No study has been made of the behaviour of type II reflections.

The experimental data can be fitted empirically to a rate law of the form $i-1 = kt$, where $i = \sqrt{I_0/I}$ and k is a constant. Such a law cannot be rationalized until a structure determination and an interpretation of the subsidiary reflections become available; however, if the process by which the subsidiary reflections decrease in intensity is one of disordering, and if the degree of long-range order α is given by an expression of the form $I/I_0 = (1-\alpha)^2$, as it is in the rather simpler case of order-disorder transitions in cubic alloys (Wilchinsky, 1944), then the rate law would represent second order kinetics for a disordering process. At 795° C. the data clearly fit the second order better than the first order law $\log i = kt$, but at other temperatures either law will fit the experimental data within the rather large limits of error imposed by the inaccuracy of intensity measurement. The nature of the problem precludes the application of more sensitive kinetic criteria for the order of reaction. Since there is no reason to suppose that any change of mechanism occurs with variation in temperature a second order law will be assumed to apply to the process (fig. 2 (i)). At temperatures investigated in the range 700° C. to 817° C. the subsidiary reflections decrease in intensity and vanish if the heating is sufficiently prolonged; they maintain their position, sharpness, and shape unchanged. Below 700° C. the rate of change of intensity was

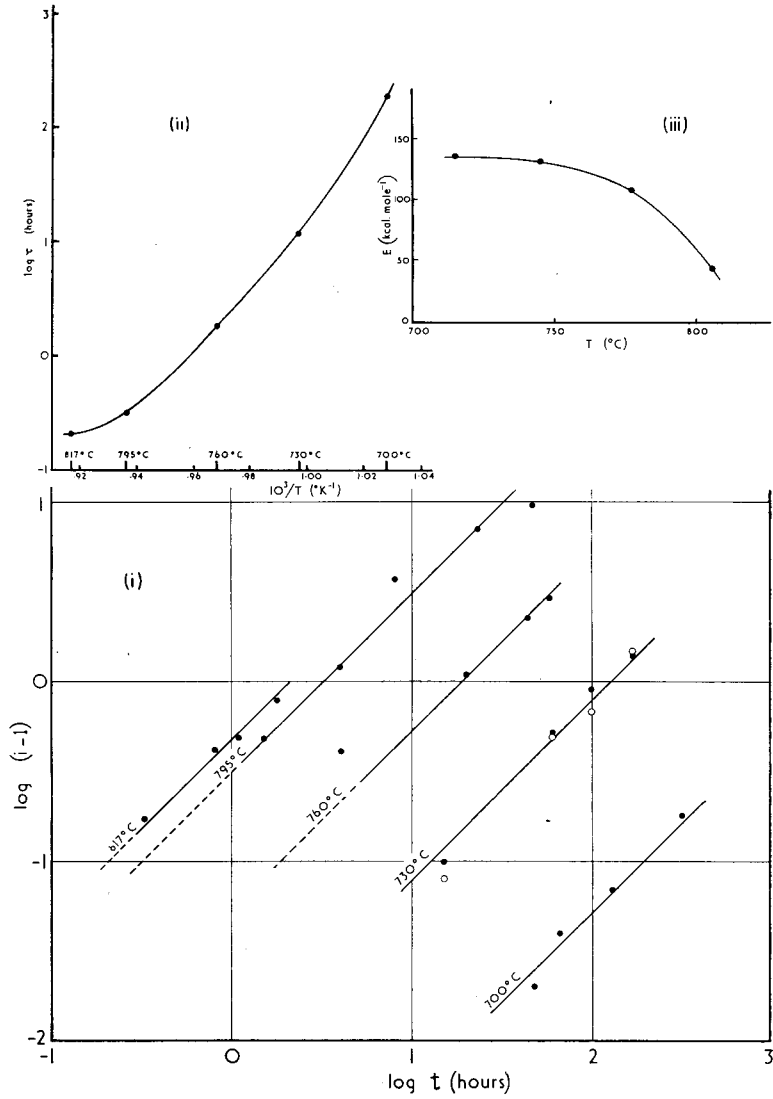


Fig. 2. (i) Plot of $i-1 = kt$; \bullet refers to $1.1 \cdot 417 \cdot \frac{1}{2}$, \circ refers to $0.1 \cdot 417 \cdot \frac{1}{2}$. (ii) Plot of $\log \tau = E/RT + B$. (iii) Plot of activation energy against temperature.

too slow for convenient observation, and at 850° C. slow decomposition of the yoderite structure had begun.

It is convenient to designate the state of yoderite without subsidiary reflections, which is stable above some critical temperature less than 700° C., as high-yoderite, and to refer to yoderite with subsidiary reflections as low-yoderite. All kinetic observations have thus been made in the region in which low yoderite is metastable, and the rate of the transformation process at 700° C. is so sluggish that it would seem that transitional thermal states corresponding to subsidiary reflections of diminished intensity are inaccessible to kinetic observation, in contrast to order-disorder transitions in certain alloys, where transitional states of partial ordering rapidly approach equilibrium. That the kinetic observations have been made for transition from a metastable to a stable state does not invalidate the conclusions drawn from those data in the next paragraph, but does preclude any inferences about the thermodynamic equilibrium between the high and low thermal states.

In considering the temperature coefficient of the rate of reaction it is convenient to assume a relationship of the form $\tau = Ae^{E/RT}$, where τ is the time required for a given fraction of the transformation to take place isothermally at T° K., i.e. the time corresponding to a given value of i , and A is a constant.¹ A plot of this expression in the form $\log \tau = B + E/RT$ is shown in fig. 2 (ii). If the observed process is an order-disorder transition, E may be taken to represent the energy barrier which an ion must surmount to pass from a position of order to become part of a disordered array. The value of E will be expected (Bragg, Sykes, and Bradley, 1937) to decrease as T rises, since each ion will then have more of its neighbours in the disordered state; such a decrease is observed (fig. 2 (iii)) from values in the region of 140 kcal. per gram-ion at 700° C. to 40 kcal. per gram-ion at 817° C.

Values of the activation energy E of the process will be independent of the correctness of any order-disorder interpretation of I/I_0 and of the right choice of rate law. Such activation energies, for which no more than approximate accuracy is claimed, should correspond to those characteristic of the diffusion of cations through a silicate lattice, since in each case momentary displacement of ions from lattice positions must occur. No comparable data are available for the diffusion of cations

¹ This expression is a form of the Arrhenius equation $k = Ae^{-E/RT}$, familiar in gas and solution kinetics, where it has a theoretical basis. It can readily be seen that $k\tau = \text{constant}$. By considering τ instead of k , uncertainty about the precise significance of i is eliminated.

